Limit Analysis of Masonry Structures Accounting for Uncertainties in Constituent Materials Mechanical Properties

Denis Benasciutti[1] and Gabriele Milani*,[2]

[1]*DIEGM, Dipartimento di Ingegneria Elettrica Gestionale Meccanica, via delle Scienze 208, 33100 Udine (Italy) and* [2]*IBK-ETHZ, Institut f. Baustatik und Konstruktion, Swiss Federal Institute of Technology, Wolfgang-Pauli-Str. 15, 8093 Zürich, Switzerland*

Abstract: The uncertainty often observed in experimental strengths of masonry constituent materials makes critical the selection of the appropriate inputs in the finite elements limit analysis of complex masonry buildings, as well as requires modeling the building ultimate load as a random variable. The most direct approach to solve limit analysis problems in presence of random input parameters is the use of extensive Monte Carlo (MC) simulations. Nevertheless, when MC methods are used to estimate the collapse load cumulative distribution of a masonry structure, large scale linear programming problems must be numerically tackled several times, so precluding the practical utilization of large scale MC simulations. To reduce the computational cost of a traditional MC approach, in the present paper direct computer calculations are replaced with inexpensive Response Surface (RS) models. In particular, RS models are utilized for the limit analysis of a masonry structure in- and out-of-plane loaded, assuming input mechanical properties as random parameters. Two different RS models are analyzed, derived respectively from small scale (20 replicates) MC and Latin Hypercube (LH) simulations. The accuracy of the estimated RS models, as well as the good estimations of the collapse load cumulative distributions obtained *via* polynomial RS models in comparison with large scale MC simulations, show how the proposed approach could be a useful tool in problems of technical interest.

Key Words: Masonry, Limit analysis, Monte carlo simulations, Latin Hypercube.

INTRODUCTION

The structural analysis of masonry buildings under seismic actions is generally a complex task, requiring complicate nonlinear analyses, performed nowadays with finite elements (FE) methods.

The collapse load of a given building is clearly a function of the geometry, of the external actions, of the materials properties and finally of the environmental conditions (humidity, temperature). In the technical literature, many different methods based on FE simulations can be found for the evaluation of the ultimate loads of engineering structures (see for instance [1-5]). A suitable way, which requires a relatively low computational cost, is the use of limit analysis theorems in combination with FE simulations. Such an approach is able to give important information at failure, as for instance collapse loads, failure mechanisms and, at least on critical sections, the stress distribution. The hypotheses at the base of the method are statically applied loads, infinite ductility and associated flow rules for the constituent materials. These hypotheses yield well for steel structures (see Olsen [4]), but it has been shown that quite reliable results can be obtained also for concrete (Olsen [6]) and masonry (Sutcliffe *et al*. [7] and Milani *et al*. [2]) materials that, as well known, exhibit a finite ductility. Nevertheless, an analysis at collapse for masonry structures remains a very difficult task, both from a theoretical and numerical point of view, essentially because brickwork is constituted by an assemblage of bricks between which thin mortar joints are laid. At present, the three approaches most utilized in practice to tackle engineering problems involving the study of masonry structures rely on micro-modeling [1, 8], macro-modeling [9] and homogenization [10]. An alternative technically meaningful methodology is finally represented by the so-called macro-elements approach presented, for instance, in [11].

While micro-modeling is limited to small structures [12], since a separate modeling of bricks and joints is required in the framework of finite elements, in macro-modeling the heterogeneous material is substituted with a macroscopic homogeneous fictitious one, obtained essentially from experimental data fitting. Despite the fact that macro-modeling is suitable for large scale structures, it requires a difficult calibration of its mechanical properties, usually obtained by means of costly experimental campaigns [13].

In light of these considerations, homogenization theory seems particularly attractive, since it is able to reproduce macroscopic masonry behavior at failure requiring only the knowledge of mechanical properties of the constitutive materials (always available with low cost), once that a suitable repetitive unitary cell is found.

In the framework of homogenization and limit analysis, for a fixed building geometry and for a given set of applied external actions, the collapse load y of a masonry structure resulting from numerical FE calculations will only depend on the input materials properties (bricks and mortar), according to the mathematical model:

$$y = h(\mathbf{x}) \tag{1}$$

*Address correspondence to this author at the Institut f. Baustatik und Konstruktion, Swiss Federal Institute of Technology (ETH), Wolfgang-Pauli-Str. 15, 8093 Zürich, Switzerland (Formerly: ENDIF, Engineering Department in Ferrara, University of Ferrara, via Saragat 1, 44100 Ferrara, Italy); E-mail: gabriele.milani@unife.it, milani@ibk.baug.ethz.ch

1874-1495/08

where vector $\mathbf{x} = (x_1, x_2, ..., x_m)$ collects all the relevant input material parameters (e.g. cohesion, friction angle, cut-off stress, joints and bricks compressive strength, etc.).

Function $h(-)$ just introduced to formalize the input/output relation of the computer FE simulation, even though highly non-linear, is strictly deterministic, i.e. replicated calculations from running the same input parameters will give the same output collapse loads.

Considering that the material strength properties of single masonry constituents (e.g. mortar, brick) determined by experimental testing often show a very large variability [1, 14, 15] selection of the appropriate values to use in numerical simulations could become a critical task. For instance, experimental data are quite often so spread, that simply using mean values could give unsafe results. In addition, the uncertainty in materials strength properties also induces a corresponding variability in the resultant collapse load. On the other hand, in building practice the so called characteristic values approach is often used. Such an approach consists in the following procedures: (1) a deterministic structural analysis for the structure at hand is performed using as material mechanical properties a single strength value corresponding to a small probability (usually 5 %, denoting material strengths characteristic values) of a Gaussian distribution (b) obtained from a very small experimental data set (for instance, 5 cubic compressive strengths in case of concrete structures). Therefore, it is clear that no information on the collapse load probability distribution can be deduced from such a unique deterministic structural analysis performed.

As a consequence, a reliable approach would require a probabilistic analysis for estimating the probability distribution of the building limit load (assigned the probability distributions of the input strength properties of single masonry constituents) and then calculating failure probabilities and safety levels.

However, explicit determination of the collapse load probability distribution needs the explicit knowledge of function $h(-)$, which unfortunately is rarely known in a closed-form.

A possible alternative is the utilization of an approximate probabilistic analysis based on extensive Monte Carlo (MC) simulations, in which sampling-based techniques are used to study how uncertainty propagates from random input parameters to the calculated analysis results, by repetitively selecting values for the random input variables and then calculating the corresponding analysis outputs. Specifically, in the MC method the input values are chosen at random from their own domains of definition, which makes the sampled values more likely to occur in regions associated to high probabilities, usually around the mean of the distribution. Hence, large sample sizes (i.e. many simulations runs) are needed to assure a reasonable coverage of the range of each input variable (and of the calculated analysis output), as well as to achieve a sufficient statistical convergence of the estimated output probability distribution.

Considering that in numerical limit analyses of complex buildings a single deterministic simulation could take many hours of calculations (see [16]), the large sample sizes used by the extensive MC simulations becomes prohibitive for practical applications.

To alleviate the overall computational cost, a possibility is to replace the MC method with improved sampling-based techniques, which guarantee the same statistical convergence with smaller sample sizes. As an example, in the last decades the Latin Hypercube (LH) method has received an increasing attention in many different research areas and applications, where the use of large samples is not computationally practicable [17-19]. However, even though the LH method can help in reducing the total number of simulation runs required, in some applications the overall simulation time could still remain unacceptably high.

A completely different approach which can drastically reduce the total computation time is to adopt the so-called response surface (RS) techniques, see Fig. (**1**), to construct a surrogate model (or metamodel), that can be used as inexpensive mathematical approximation of the actual, yet time-consuming, computer simulation [20-24]. More precisely, the true, but generally unknown, function $h(-)$ introduced in Eq. (1), formalizing the input/output relationship of a FE limit analysis, is replaced by an approximation $\hat{h}(-)$, which is calibrated on observed outputs $y_{c,k} = h(\mathbf{x}_{c,k})$, resulting from running computer calculations on a small set of optimally selected design input points $\mathbf{x}_{c,k}$.

Assumed that the overall approximation error is sufficiently small and technically acceptable, the decisive advantage of RS techniques is that the sample sizes required for an accurate calibration are significantly lower (e.g. two order of magnitude) than those used in extensive MC simulations.

Once the RS model has been calibrated, it can be used as a proxy of direct computer calculations in extensive MC simulations, which are used to generate large sets analysis outputs used to estimate the output probability distribution.

Different RS models exist, which differ in respect to their relative accuracy and complexity. Even though many studies have investigated what combination of design scheme and RS technique would give the best level of accuracy, no general rules were found for all engineering problems [20-22, 24]. On the other hand, other aspects than accuracy were indicated as equally important: robustness (accuracy and stability through different types of problems), efficiency (computational effort required in metamodel calibration), transparency (existence of explicit relationships between inputs and outputs) and conceptual simplicity (easiness of implementation). As an example, the classical polynomial RS approximation was indicated as the optimal choice due to its great simplicity and possible fairly good accuracy [21].

With the aim of investigating the potentiality of polynomial RS models in replacing actual computer simulations in the homogenized limit analysis of complex masonry buildings with random input parameters, this work will attempt:

1. to investigate the accuracy and efficiency of polynomial RS models as inexpensive replacement of direct computer simulations;

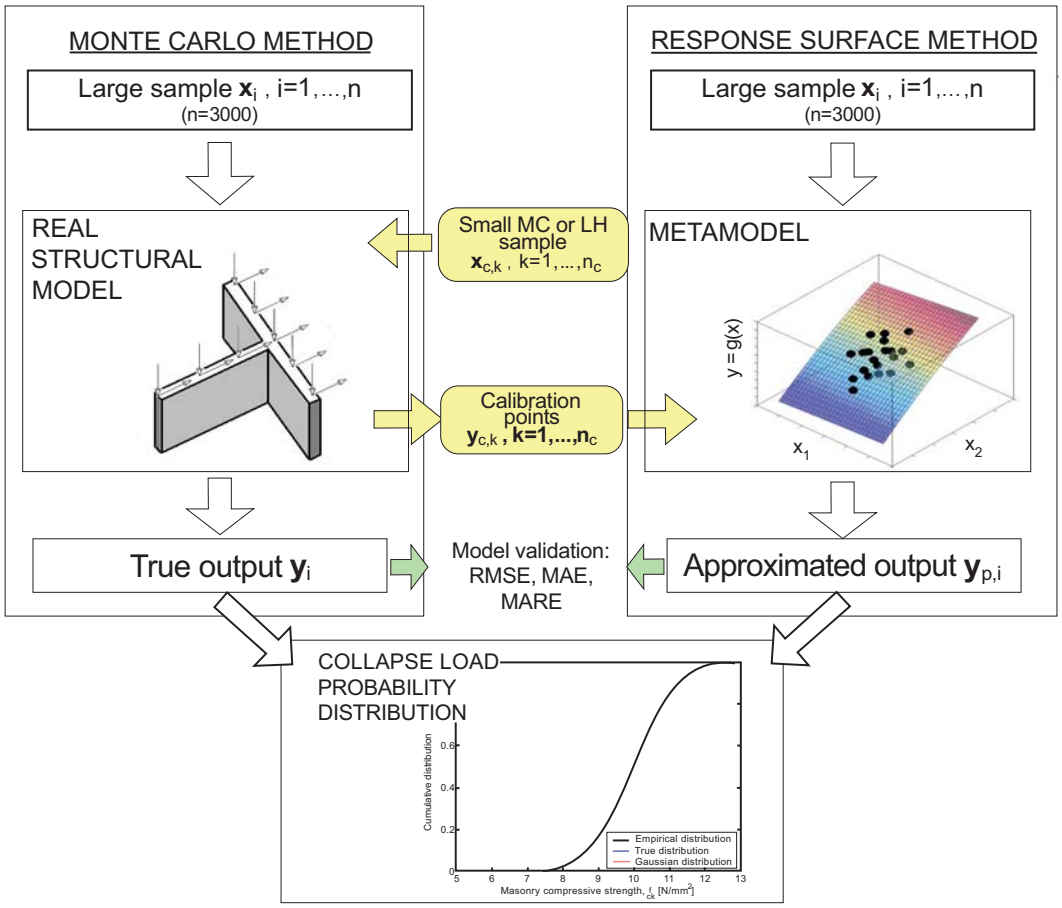

Fig. (1). Schematic representation of extensive Monte Carlo simulations (*via* direct computer calculations or *via* RS model) used to estimate the collapse load probability distribution. Construction and validation of the polynomial RS model is also shown.

2. to study the correlation between RS accuracy and design scheme, by referring to the MC and the LH techniques for generating input points for RS fitting;
3. to evaluate the accuracy of the estimated output probability distribution when polynomial RS models are used in place of direct computer calculations in extensive MC simulations.

The utilization of limit analysis in combination with RS approximation seems particularly adequate, being related to the fact that the response of limit analysis is smooth with respect to variation of the material parameters. Obviously, the extension of this statement to experimentally observed data is, in principle, not possible since due to the practical impossibility to perform extensive experimental MC tests on real scale masonry structures.

Numerical simulations concerning an example of relevant technical interest of an in- and out-of-plane loaded masonry wall is presented.

First, a quadratic polynomial RS model is constructed on a small set of observed analysis outputs $y_{c,k}$, resulting from running computer simulations on a small set of input points $\mathbf{x}_{c,k}$ (at most 20 or 30), generated by either the MC method or the LH technique.

The estimated polynomial RS model is then used as a proxy of direct computer calculations in extensive MC simulations with large sample sizes (equal to 3000), used to assess the collapse load probability distribution. The sample sizes of large MC samples were chosen as a necessary compromise between the high computational cost of all numerical simulations and the required accuracy in the estimate of the collapse load probability distribution, as well as considering 0.5% as a sufficient value for the failure probability in technical applications. On the other hand, considering the large variability of input material properties due to usually scarce experimental tests, higher sample size would unnecessarily increase the overall computational cost, without improving the accuracy of the tail estimates of the collapse load probability distribution.

A comparison between the probability distribution estimated *via* RS model and the one obtained by direct computer calculations is presented.

The same large MC samples are also used as validation points to compare the fitting performance of RS models constructed from MC or LH design points.

The presented results show how the use of polynomial RS with MC simulations can drastically reduce the overall computation time, while providing acceptable levels of accuracy, which assures quite good estimates of the collapse load probability distribution.

MASONRY HOMOGENIZED FAILURE SURFACES

Failure loads of complex 3D masonry structures can be obtained with a relatively low computational cost by means

of a recently presented FE limit analysis approach [10], in which masonry failure surface is obtained through a micro-mechanical model which bases on homogenization theory applied in the rigid-plastic case.

A detailed description of the equilibrated micro-mechanical model adopted is reported in [1, 3, 10] and the reader is referred there for an exhaustive discussion. In this section, only the basic idea of the model proposed is recalled in order to show how FE homogenized limit analysis Monte Carlo simulations have been performed at a structural level.

In, Fig. (**2**-**a**), masonry wall Ω constituted by a periodic arrangement of bricks and mortar disposed in running bond texture is reported. Following the general procedure proposed by Suquet in [25], homogenization techniques combined with limit analysis can be used for the evaluation of masonry homogenized strength domain S^{hom} for combined in- and out-of-plane loads. In the framework of the lower bound limit analysis theorem (i.e. assuming associated flow rules for the constituent materials and imposing equilibrium equations and admissibility conditions), it can be shown that the frontier ∂ of S^{hom} is obtained solving the following linear programming problem (see also Fig. (**2**)):

$$\partial S^{\text{hom}} = \left\{ \max(\mathbf{M},\mathbf{N}) \,|\, \left\{ \begin{array}{ll} \mathbf{N} = \dfrac{1}{|Y|} \displaystyle\int_{Y\times\left[-\frac{h}{2}\ \frac{h}{2}\right]} \boldsymbol{\sigma} dV & (a) \\ \mathbf{M} = \dfrac{1}{|Y|} \displaystyle\int_{Y\times\left[-\frac{h}{2}\ \frac{h}{2}\right]} y_3 \boldsymbol{\sigma} dV & (b) \\ div\boldsymbol{\sigma} = \mathbf{0} & (c) \\ [[\boldsymbol{\sigma}]]\mathbf{n}^{\text{int}} = \mathbf{0} & (d) \\ \boldsymbol{\sigma}\mathbf{n} \quad \text{anti-periodic} \quad \text{on} \quad \partial Y_l & (e) \\ \boldsymbol{\sigma}(\mathbf{y}) \in S^m \quad \forall \mathbf{y} \in Y^m \,;\, \boldsymbol{\sigma}(\mathbf{y}) \in S^b \quad \forall \mathbf{y} \in Y^b & (f) \end{array} \right. \right\} \tag{2}$$

In the previous equation the following symbols have been used:

- $\mathbf{N}$ and $\mathbf{M}$, which represent macroscopic in-plane (membrane forces) and out-of-plane (bending moments and torsion) tensors;

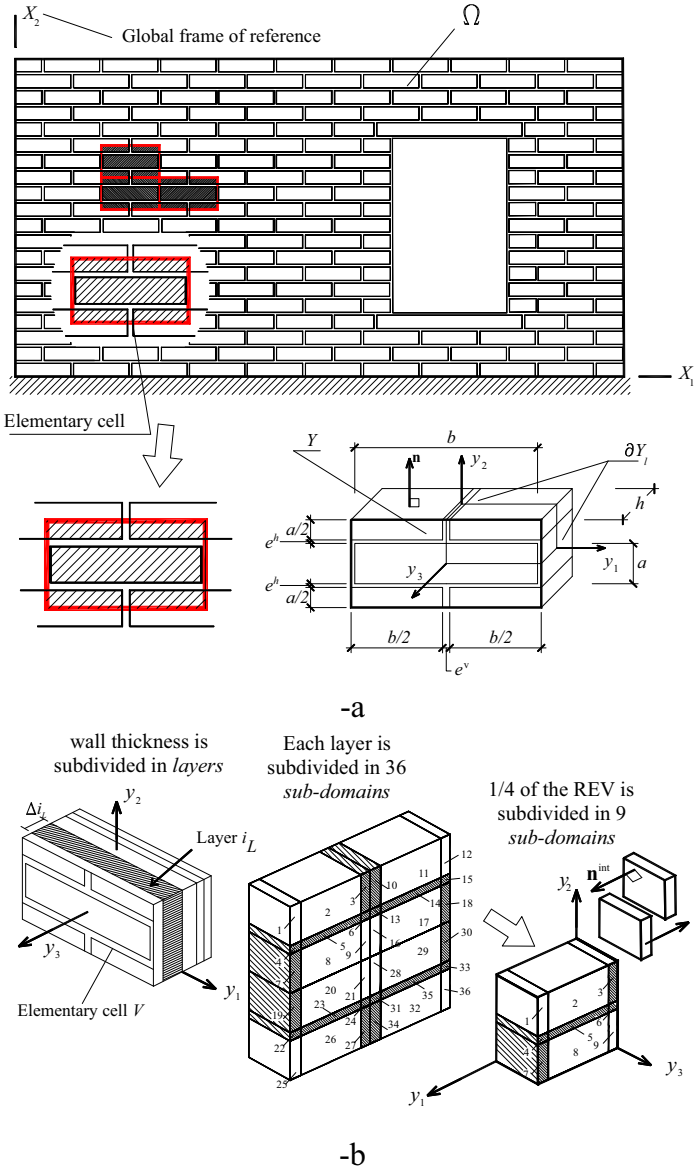

Fig. (2). Proposed micro-mechanical model. -**a**: elementary cell identification. -**b**: subdivision of the elementary cell in layers along thickness and subdivision of each layer in sub-domains.

- $\boldsymbol{\sigma}$, which is the projection of the local stress tensor along directions y_1 and y_2, see Fig. (**2**);
- $\mathbf{n}$, the outward unit vector orthogonal to ∂Y_l surface, Fig. (**2-a**);
- ∂Y_l, which is the internal boundary of the elementary cell, Fig. (**2-a**);
- $[[\boldsymbol{\sigma}]]$, representing the jump of micro-stresses across any discontinuity surface of normal $\mathbf{n}^{\text{int}}$, Fig. (**2-b**);
- S^m and S^b, denoting respectively the strength domains of mortar and bricks;
- Y, which is the cross section of the 3D elementary cell with $y_3 = 0$ (see Fig. (**2**), $|Y|$ is its area, V is the elementary cell volume, h represents the wall thickness and $\mathbf{y} = (y_1 \quad y_2 \quad y_3)$ is the position of a point in the local frame of reference.

As shown in Fig. (**2-b**), in the model the unit cell is sub-divided into a fixed number of layers along its thickness. For each layer out-of-plane components σ_{i3} $(i = 1, 2, 3)$ of the micro-stress tensor $\boldsymbol{\sigma}$ are set to zero (i.e. a typical plane stress condition for each layer is adopted), so that only in-plane components σ_{ij} $(i, j = 1, 2)$ are considered active. Furthermore, σ_{ij} $(i, j = 1, 2)$ are kept constant along the thickness Δ_{i_L} of each layer, i.e. in each layer $\sigma_{ij} = \sigma_{ij}(y_1, y_2)$. For each layer, each fourth of the representative volume element is sub-divided into nine geometrical elementary entities (sub-domains), so that the entire elementary cell is sub-divided into 36 sub-domains (see [10] and Fig. (**2-b**) for further details).

For each sub-domain k and layer i_L, polynomial distributions of degree (m) in the variables (y_1, y_2) are a priori assumed for the stress components. Since stresses are polynomial expressions, the generic ij th component can be written as follows:

$$\sigma_{ij}^{(k,i_L)} = \mathbf{X}(\mathbf{y})\mathbf{S}_{ij}^{(k,i_L)T} \qquad \mathbf{y} \in Y^{(k,i_L)} \tag{3}$$

Where:

- $\mathbf{X}(\mathbf{y}) = [1 \quad y_1 \quad y_2 \quad y_1^2 \quad y_1 y_2 \quad y_2^2 \quad \ldots]$
- $Y^{(k,i_L)}$ represents the k th sub-domain of layer (i_L)
- $\mathbf{S}_{ij}^{(k,i_L)} = [S_{ij}^{(k,i_L)(1)} \quad S_{ij}^{(k,i_L)(2)} \quad S_{ij}^{(k,i_L)(3)} \quad S_{ij}^{(k,i_L)(4)} \quad S_{ij}^{(k,i_L)(5)} \quad S_{ij}^{(k,i_L)(6)} \quad \ldots]$

is a vector representing the unknown stress parameters of sub-domain k of layer i_L.

The imposition of equilibrium inside each sub-domain, the continuity of the stress vector on interfaces and the anti-periodicity of $\boldsymbol{\sigma}\mathbf{n}$ permits a strong reduction in the number of independent stress parameters (see [10] for further details), allowing to write the stress vector $\tilde{\boldsymbol{\sigma}}^{(k,i_L)}$ of layer i_L inside each sub-domain as $\tilde{\boldsymbol{\sigma}}^{(k,i_L)} = \mathrm{X}^{(k,i_L)}(\mathrm{y})\ \tilde{\mathrm{S}}^{(i_L)}$ where $\tilde{\mathbf{S}}^{(i_L)}$ is the vector of linearly independent unknown stress parameters of layer i_L, k is a sub-domain and $\tilde{\mathbf{X}}^{(k,i_L)}$ is a $3\mathrm{x}\, n_s$ matrix, which depends only on the geometry of the sub-domain (n_s is the length of vector $\tilde{\mathbf{S}}^{(i_L)}$).

Once that an equilibrated polynomial field in each layer is obtained (here fourth-order polynomials are used), the proposed in- and out-of-plane model requires a subdivision of the wall thickness into n_L layers (Fig. (**2-b**), with a constant thickness $\Delta_{i_L} = h / n_L$. This allows to derive the following simple non-linear optimization problem:

$$\max\{\lambda\}$$

$$\partial S^{\text{hom}} \equiv \left\{ \text{such that} \left\{ \begin{array}{ll} \tilde{\mathbf{N}} = \int_{k,i_L} \tilde{\boldsymbol{\sigma}}^{(k,i_L)}\, dV & (a) \\ \tilde{\mathbf{M}} = \int_{k,i_L} \tilde{\boldsymbol{\sigma}}_{\mathrm{y}_3}^{(k,i_L)}\, dV & (b) \\ \sum = [\tilde{\mathbf{N}} \quad \tilde{\mathbf{M}}] = \lambda \mathbf{n}_\Sigma & (c) \\ \tilde{\boldsymbol{\sigma}}^{(k,i_L)} = \tilde{\mathbf{X}}^{(k,i_L)}(\mathbf{y})\tilde{\mathbf{S}}^{(i_L)} & (d) \\ \tilde{\boldsymbol{\sigma}}^{(k,i_L)} \in S^{(k,i_L)} & (e) \\ k = 1,\ldots,\ \text{number of } \textit{sub - domains} & (f) \\ i_L = 1,\ldots,\ \text{number of sub - } \textit{layers} & (g) \end{array} \right. \right. \tag{4}$$

In equation (4) λ represents the so-called load multiplier, $S^{(k,i_L)}$ denotes the non-linear strength domain of the constituent material (mortar or brick) corresponding to the k th sub-domain and i_L th layer. As a rule, λ is an ultimate moment, an ultimate membrane action or a combination of moments and membrane actions. In order to recover ∂S^{hom} surface point by point, a fixed direction $\mathbf{n}_\Sigma$ in the six dimensional space of membrane actions ($\tilde{\mathbf{N}} = [N_{xx} \ N_{xy} \ N_{yy}]$) and bending + torsion moments ($\tilde{\mathbf{M}} = [M_{xx} \ M_{xy} \ M_{yy}]$) is chosen. For each $\mathbf{n}_\Sigma$, a failure load λ at a cell level is computed. The knowledge of $\mathbf{n}_\Sigma$ and λ permits to find a point of the masonry failure surface in six dimensions. Changing the direction $\mathbf{n}_\Sigma$, a new λ is calculated from the optimization problem, hence a new point of the failure surface is collected. In this manner, repeating the procedure for a suitable number of different directions, several points of ∂S^{hom} can be calculated. With the hypotheses assumed in [10] ∂S^{hom} results convex. Therefore, a final Delaunay tessellation permits to find a lower bound linear approximation of ∂S^{hom}.

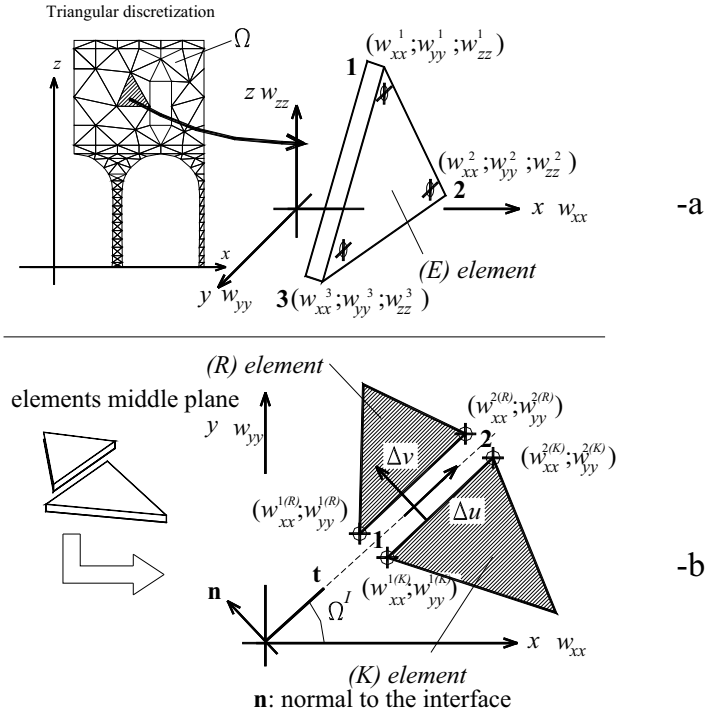

Fig. (3-a). Triangular plate and shell element used for the upper bound FE limit analysis. -**b**: discontinuity of the in-plane velocity field.

A linearization with 80 planes of such failure surface is implemented in the FE limit analysis code described in the following section, for performing the upper bound homogenized limit analyses presented in this paper.

Of course, the failure surface obtained with the homogenization procedure presented above depends on both mechanical properties assumed for joints and bricks; therefore, also the collapse load of the structures considered in Example 2 and 3 of this paper indirectly depends on both bricks and mortar mechanical properties. Finally, it is worth noting that, in principle, also fracture energy of constituent materials should be ideally considered as a random variable (see [15]), although in limit analysis fracture energy effect is disregarded.

3D KINEMATIC FE LIMIT ANALYSIS

The upper bound approach developed in this paper is fully described in [3] and the reader is referred there for a detailed description of the numerical model. Here, only the bases of the procedure proposed are reported. The formulation uses three noded triangular elements with linear interpolation of the velocity field inside each element, so that three velocity unknowns per node i, say w_{xx}^i , w_{yy}^i and w_{zz}^i (respectively 2 in-plane velocities and 1 out-of-plane velocity, see Fig. (**3-a**) are introduced for each element E, meaning that the velocity field is linear inside an element.

A possible jump of velocities on interfaces between adjoining elements is supposed to occur, with linear interpolation of the jump along the interface. The introduction of a jump of displacements is useful to obtain reliable collapse loads for friction materials (see [5]). In this framework, for each interface between coplanar adjacent elements, four additional unknowns are introduced ($\Delta\mathbf{u}^I = \left[\Delta v_1\ \Delta u_1\ \Delta v_2\ \Delta u_2\right]^T$), representing the normal (Δv_i) and tangential (Δu_i) jumps of velocities (with respect to the discontinuity direction) evaluated on nodes $i = 1$ and $i = 2$ of the interface (see Fig. (**3-b**)). For any pair of nodes on the interface between two adjacent and coplanar triangles R and K, the tangential and normal velocity jumps can be written in terms of the Cartesian nodal velocities of elements R - K (see Fig. (**3**) for details), so that a system of four linear equations in the form $\mathbf{A}_{11}^{eq}\mathbf{w}^R + \mathbf{A}_{12}^{eq}\mathbf{w}^K + \mathbf{A}_{13}^{eq}\Delta\mathbf{u}^I = \mathbf{0}$ can be written, being $\mathbf{w}^R$ and $\mathbf{w}^K$ the 9×1 vectors that collect velocities of elements R and K respectively and $\mathbf{A}_{1j}^{eq}$ $j = 1,2,3$ matrices which depend only on the interface orientation Ω^I (Fig. (**3**)).

Since velocities interpolation is kept linear inside each triangular element, only three equality constrains representing the plastic flow in continuum (obeying an associated flow rule) are introduced for each element in the form $\dot{\boldsymbol{\varepsilon}}_{pl}^E = \dot{\lambda}^E \partial S^{\text{hom}} / \partial \boldsymbol{\Sigma}$, where $\dot{\boldsymbol{\varepsilon}}_{pl}^E$ is the plastic strain rate vector of element E, $\dot{\lambda}^E \geq 0$ is the plastic multiplier, S^{hom} is the homogenized (non) linear failure surface of masonry in the six dimensional space of membrane N_{11}, N_{12}, N_{22} and bending M_{11}, M_{12}, M_{22} actions, i.e. $\boldsymbol{\Sigma} = (N_{11}, N_{12}, N_{22}, M_{11}, M_{12}, M_{22})$.

For each element, plastic flow in continuum may be written in the form $\mathbf{A}_{11}^{eq}\mathbf{w}^E + \mathbf{A}_{12}^{eq}\dot{\boldsymbol{\lambda}} = \mathbf{0}$, where $\mathbf{w}^E$ is the

vector of element velocities and $\dot{\boldsymbol{\lambda}}^E$ is a $m \times 1$ vector of plastic multiplier rates, one for each plane of the linearized failure surface.

Denoting with $\mathbf{w}_{zz,E} = \begin{bmatrix} w_{zz}^{i(E)} & w_{zz}^{j(E)} & w_{zz}^{k(E)} \end{bmatrix}^T$ the element E out-of-plane nodal velocities and with $\dot{\boldsymbol{\theta}}_E = \begin{bmatrix} \dot{\vartheta}_i^E & \dot{\vartheta}_j^E & \dot{\vartheta}_k^E \end{bmatrix}$ the side normal rotation rates, it is possible to show that $\dot{\boldsymbol{\theta}}_E$ and $\mathbf{w}_{zz,E}$ are linked by the compatibility equation (Fig. (**4**)) $\dot{\boldsymbol{\theta}}_E = \mathbf{B}_E \mathbf{w}_{zz,E}$, where $\mathbf{B}_E$ is a 3x3 matrix that depends only on the geometry of element E.

The total internal power dissipated P^{in} is constituted by the power dissipated in continuum, P_E^{in}, and the power dissipated on interfaces, P_I^{in}. It is interesting to note that out-of-plane plastic dissipation occurs only along each interface I between two adjacent triangles R and K or on a boundary side B of an element Q (see Fig. (**4**)). Therefore P_E^{in} can be evaluated for each triangle E of area A_E taking into account only in-plane actions.

Let us assume that a linear approximation (with m hyper-planes) of masonry failure surface in the form $S^{\text{hom}} \equiv \mathbf{A}^{in} \boldsymbol{\Sigma} \leq \mathbf{b}^{in}$ is at disposal solving, as already discussed in the previous Section, a number of linear programming problems (4). Here, $\mathbf{A}^{in}$ is a $m \times 6$ matrix of coefficients of each hyper-plane and $\mathbf{b}^{in}$ is a $m \times 1$ vector of the right hand sides of the linear approximation.

As the homogenized (linearized) failure surface is constituted by m hyper-planes of equation $A_{xx}^q N_{xx} + A_{yy}^q N_{yy} + A_{xy}^q N_{xy} + B_{xx}^q M_{xx} + B_{yy}^q M_{yy} + B_{xy}^q M_{xy} = C_E^q$, with $1 \leq q \leq m$, an estimation of P_E^{in} can be easily obtained as $P_E^{in} = A_E \sum_{q=1}^{m} C_E^q \dot{\lambda}_E^{(q)}$ with curvature rate tensor equal to zero, being $\dot{\lambda}_E^{(q)}$ the plastic multiplier rate of the triangle E associated to the qth hyper-plane of the linearized failure surface.

On the other hand, for an interface I between adjoining elements of length Γ and orientation Ω^I, a rotation operator is applied to the linearized homogenized admissible domain frontier in order to obtain with a limited computational effort m equations (one for each hyper-plane) in the form $A_{tt}^q N_{tt} + A_{nn}^q N_{nn} + A_{tn}^q N_{tn} + B_{tt}^q M_{tt} + B_{nn}^q M_{nn} + B_{tn}^q M_{tn} = C_I^q$ representing $\partial \widetilde{S}^{\text{hom}}$ in the $\mathbf{n} - \mathbf{t}$ interface frame of reference, defined in Fig. (**3**).

In this way, the power dissipated P_I^{in} along an interface I can be easily estimated as reported by Krabbenhoft *et al.* [26] and the reader is referred there for a detailed discussion of the kinematic hypotheses adopted for the evaluation of P_I^{in}.

After some assemblage operations (see for instance [4, 14, 26]), the following linear programming problem is obtained, where the objective function is the total internal power dissipated:

$$\min \left\{ \sum_{I=1}^{n^I} P_I^{in} + \sum_{E=1}^{n^E} P_E^{in} - \mathbf{P}_0^T \mathbf{w} \right\}$$

$$\text{such that} \begin{cases} \mathbf{A}^{eq} \mathbf{U} = \mathbf{b}^{eq} \\ \dot{\boldsymbol{\lambda}}^{I,ass} \geq \mathbf{0} \quad \dot{\boldsymbol{\lambda}}^{E,ass} \geq \mathbf{0} \\ \dot{\boldsymbol{\lambda}}^{ass} = \dot{\boldsymbol{\lambda}}^{+} - \dot{\boldsymbol{\lambda}}^{-} \\ \dot{\boldsymbol{\lambda}}^{+} \geq \mathbf{0} \quad \dot{\boldsymbol{\lambda}}^{-} \geq \mathbf{0} \end{cases} \tag{5}$$

In equation (5) the following symbols are used:

- $\mathbf{U}$ is the vector of global unknowns and collects the vector of assembled nodal velocities ($\mathbf{w}$), the vector of assembled element plastic multiplier rates ($\dot{\boldsymbol{\lambda}}^{E,ass}$), the vector of assembled jump of velocities on interfaces ($\Delta \mathbf{u}^{I,ass}$), the vector of assembled interface plastic mul-

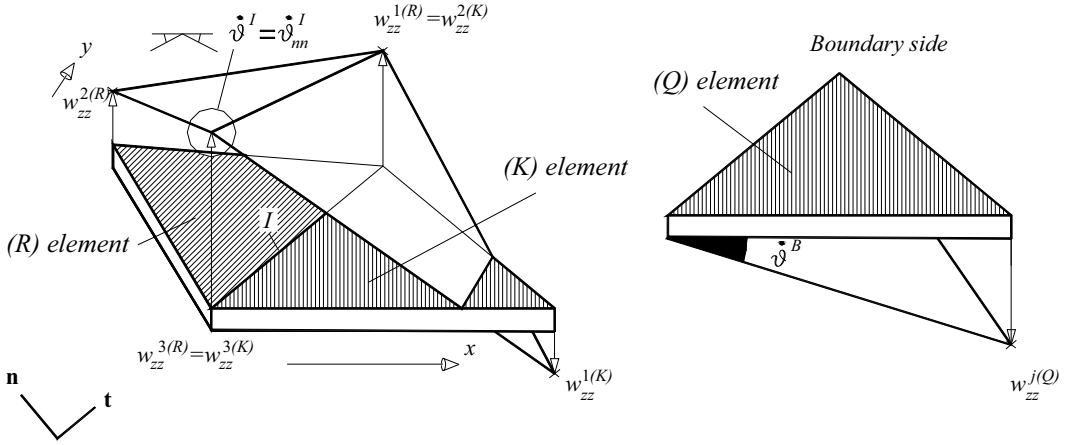

Fig. (4). Rotation along an interface between adjacent triangles or in correspondence of a boundary side.

tiplier rates ($\dot{\boldsymbol{\lambda}}^{I,ass}$) and the vector of interface and boundary out-of-plane rotation rates $\dot{\boldsymbol{\lambda}}^{ass}$.

- $\mathbf{A}^{eq}$ is the overall constraints matrix and collects normalization conditions, velocity boundary conditions, relations between velocity jumps on interfaces and elements velocities, constraints for plastic flow in velocity discontinuities and constraints for plastic flow in continuum.
- n^E and n^I are the total number of elements and interfaces, respectively.
- $\mathbf{P}_0$ is the vector of (equivalent nodal) permanent loads.

POLYNOMIAL RESPONSE SURFACE (RS) MODELING

Given the vector $\mathbf{x}_i$ of analysis inputs for the ith computer simulation, a quadratic polynomial RS model has the form:

$$y_{\mathrm{p},i} = c_0 + \sum_{q=1}^{m} c_q\, x_{i,q} + \sum_{q=1}^{m}\sum_{r=q}^{m} c_{qr}\, x_{i,q}\, x_{i,r} \qquad (6)$$

where m is the total number of input variables (i.e. random material properties), $x_{i,q}$ is the value of the qth input variable for the ith computer run and c_q are (unknown) coefficients.

Given n independent observed analyses outputs y_i, $i = 1,...,n$, the estimation problem can be formulated in compact matrix notation as:

$$\mathbf{y} \approx \mathbf{X}\hat{\mathbf{c}} \qquad (7)$$

where $\mathbf{y}$ is the vector of observed outputs, $\mathbf{X}$ is the so called design matrix, while the unique least-squares estimator of the unknown coefficients is:

$$\hat{\mathbf{c}} = \left(\mathbf{X}^T\mathbf{X}\right)^{-1}\mathbf{X}^T\mathbf{y} \qquad (8)$$

A RS model is fitted on a set $y_{\mathrm{c},k}$, $k = 1,...,n_{\mathrm{c}}$ of observed analysis outputs, derived from computer calculations on a set of optimally selected values $\mathbf{x}_{\mathrm{c},k}$ for the relevant input variables. Different design of experiments strategies can be used to sample the input variables for RS fitting [27].

Several studies in the literature, in trying to discover what design of experiment would provide the best accuracy, found that no method has been recognized as the best one [22, 23] and one should always refer to the specific problem under study [22, 24], although according to Simpson *et al*. [23] the basic requirement for an experimental design in deterministic computer analyses is space filling.

In the present work, the input design points are generated by two different sampling schemes: classical MC method and the LH technique, the latter being considered for its relative simplicity with respect to other existing techniques, and because it provides a better space filling compared to the MC method.

Experimental design: Monte Carlo and Latin Hypercube method

In the classical MC method, the input design random variables are selected at random from their domains of definition, hence the sampled values have more probability to occur in regions with higher probabilities (e.g. close to the mean value of the distribution).

To assure a more uniform sampling from the interval of each random variable the LH technique has been proposed as an improvement to the classical MC method [17, 19]. In the LH method, to obtain a sample of size n_{c} by m input random variables $\mathbf{x} = (x_1, x_2,..., x_m)$, we first divide the definition domain of each variable in n_{c} disjoint intervals of equal probability, according to the corresponding probability distribution of each variable. Then, we extract a sample value from each interval, leading to a set of n_{c} sampled values for each variable. Compared to the classical MC method, the LH design assures that each of the input random variables has all portions of its range represented, thus providing a more uniform sampling of the input design space. Finally, the n_{c} samples for vector $\mathbf{x}$ are obtained by combining all values previously sampled according to n_{c} random permutations. Special techniques are used to impose desired correlations among several variables, see Refs. [17, 28, 29].

VALIDATION OF FITTED RS MODEL

To quantify the prediction accuracy of an estimated RS model we calculate at n specified validation points the difference between the true analysis output y_i from a direct computer simulation and the value $y_{\mathrm{p},i}$ predicted by the polynomial RS model. Following some existing references [22, 24, 30], we refer to the Root Mean Square Error:

$$RMSE = \sqrt{\frac{1}{n}\sum_{i=1}^{n}\left(y_i - y_{\mathrm{p},i}\right)^2} \qquad (9)$$

to the Mean Absolute Error:

$$MAE = \frac{1}{n}\sum_{i=1}^{n}\left|\frac{y_i - y_{\mathrm{p},i}}{y_i}\right| \qquad (10)$$

and to the Maximum Absolute Relative Error:

$$MARE = \max\left(\left|\frac{y_i - y_{\mathrm{p},i_i}}{y_i}\right|_{i=1,...,n}\right) \qquad (11)$$

Note that while RMSE and MAE provide an average measure of the overall and local prediction accuracy, respectively, MARE quantifies the absolute worst relative prediction error.

In order to capture the trend of the prediction error as a function of the observed output values y_i, in addition to the errors introduced above we also consider the percentage relative error:

$$err_i(\%) = 100\cdot\left(\frac{y_i - \hat{y}_i}{y_i}\right) \qquad (12)$$

For each fitted RS model a value of RMSE, MAE and MARE error metrics is obtained, as well as a set of percentage relative errors, which depend on the particular set of MC

and LH calibration points used to construct the RS model, and also on the particular set of validation points considered. In fact, due to the random sampling technique adopted to generate calibration points, different MC or LH small replicated samples lead, in general, to different polynomial RS models (even with the same degree). On the other hand, the authors experienced that the use of MC and LH sampling performs better with respect to the use of a simple regular input grid, as a consequence of the over fitting polynomial approximation, see Ref. [20].

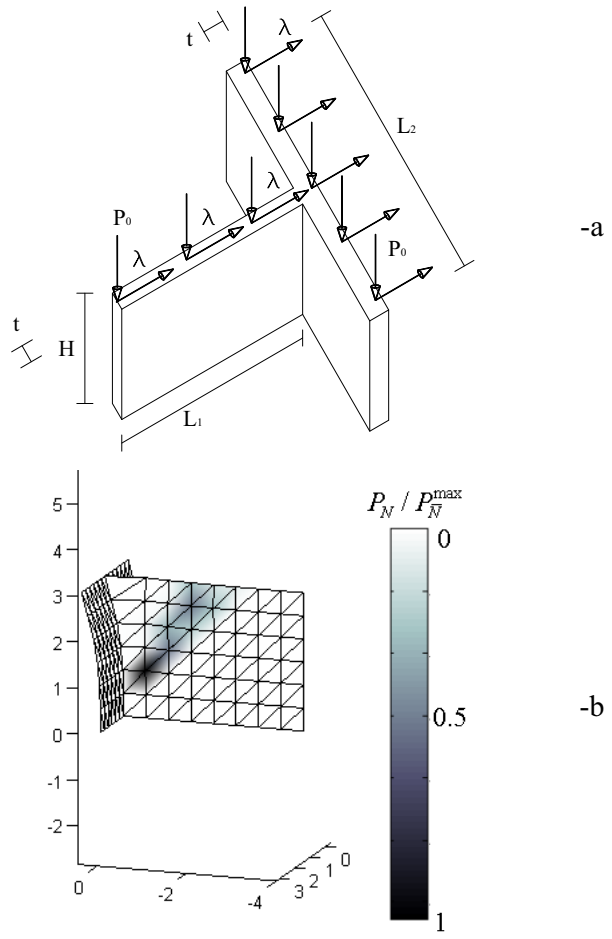

Fig. (5). Perpendicular masonry walls subjected to horizontal action. Geometry (-a) and mesh used (-b). A typical de
at collapse obtained by means of the limit analysis FE procedure adopted is also reported (P_N is the in-plane plastic dissipation evaluated at node N and $\bar{N}$ is the node of maximum dissipation).

NUMERICAL SIMULATIONS: AN EXAMPLE OF TECHNICAL INTEREST

A meaningful example of practical interest is examined in this section with the aim of illustrating the use of polynomial RS models as a computationally inexpensive alternative to direct computer calculations in extensive MC simulations, used to estimate the collapse load probability distribution of masonry buildings having random material properties.

Let us consider two perpendicular masonry walls of dimensions $L_1 = 500\,\text{cm}$, $L_2 = 300\,\text{cm}$, $H = 300\,\text{cm}$, $t = 30\,\text{cm}$ and with perfect interlocking, as shown in Fig. (**5**). Such walls are subjected to a constant vertical load due to typical dead and live loads assumed equal to $P_0 = 120$ N/mm and an increasing horizontal load depending on a load multiplier $y = \lambda$, simulating an equivalent static seismic action.

Several homogenized limit analyses FE simulations are performed on the structure by means of the triangular discretization shown in Fig. (**5-b**). Masonry is supposed constituted by Italian common bricks of dimensions 250 mm × 120 mm × 55 mm disposed in running bond texture, with joints thickness equal to 10 mm.

We assume for joints a Mohr-Coulomb failure criterion with cohesion c and friction angle $\tan(\Phi)$ both modeled as independent normally distributed random variables, with mean and standard deviation (listed as bold numbers in Table **1**) deduced from some experimental data reported in Ref. [15].

As a first step, a polynomial RS model is fitted on a small set of n_c observed collapse load values $y_{c,k}$, obtained from $\mathbf{x}_{c,k}$ input values sampled by either the MC method or the LH technique, see Fig. (**1**). More precisely, for each input pair $(c_i, \tan(\Phi_i))$, a 3D homogenized limit analysis is performed, so obtaining a set of n_c collapse loads y_i, used to construct a polynomial RS model. As suggested in [21], the number n_c of calibration points can be correlated to the number of input random variables; in our example, n_c equals 20 since only two input variables are taken into account. The independence among input random variables for LH samples is imposed by the procedure described in Ref. [29]. An example of fitted RS model with the set of LH calibration points is shown in Fig. (**6**).

As a second step, the fitted RS model is used in place of direct computer simulations in extensive MC simulations with large sample sizes (3000). The size of large MC samples was chosen as a necessary compromise between the high computational cost of all numerical simulations and the required accuracy in the estimate of the collapse load probability distribution, as well as considering 5% as a sufficient value for the failure probability in technical applications. On the other hand, considering the large variability of input material properties due to usually scarce experimental tests, higher sample size would unnecessarily increase the overall computational cost, without improving the accuracy of the tail estimates of the collapse load probability distribution.

As can be seen in Table **1**, there is a quite good agreement between the theoretical mean and standard deviation with those calculated on each large MC sample, which confirms the correctness of the sizes adopted for large MC samples.

In the third step, the n collapse load values y_i, $i = 1,...,n$ resulting from large MC simulations are used to compute the empirical cumulative distribution [31]:

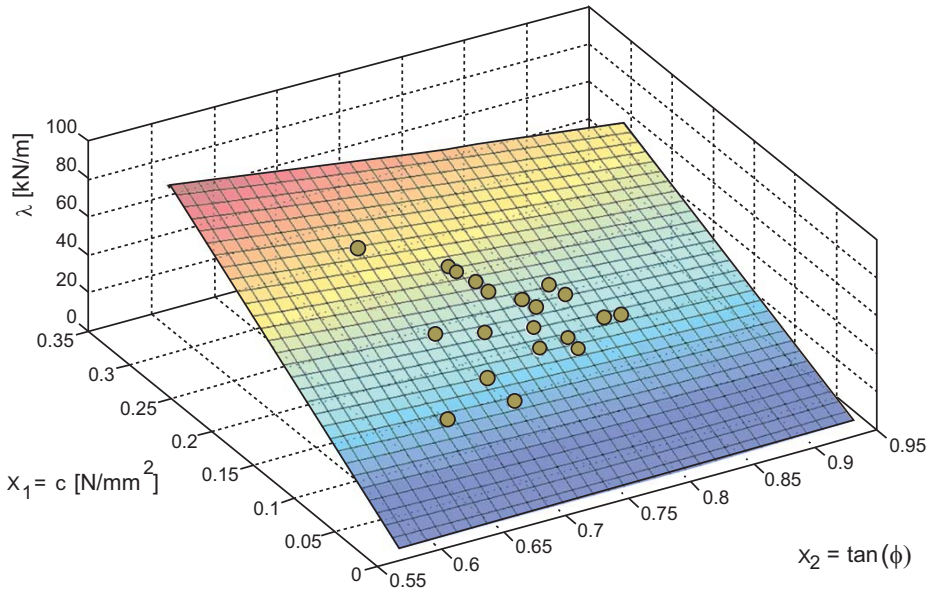

Fig. (6). Polynomial RS model with the 20 LH calibration points.

$$\hat{P}(y) = \sum_{i=1}^{n} u(y - y_i) \tag{13}$$

(where $u(x) = 1$ for $x > 0$ and zero elsewhere is an indicator function) which is an estimator of the collapse load probability distribution $P(y)$. Note that $\hat{P}(y)$ depends on the particular MC outputs y_i considered, hence it is affected by a statistical uncertainty. Replicated MC simulations are then used to estimate a mean empirical cumulative distribution [17]:

Table 1. Theoretical Mean and Standard Deviation (Bold Numbers) of the Random Input Parameters Compared with Those Calculated on the Three Large MC Samples

	Cohesion [N/mm^2]	**Tangent of Friction Angle [–]**
	$x_1 = c$	$x_2 = \tan(\Phi)$
Mean value[a]	**0.1457**	**0.75**
	0.143	0.753
	0.143	0.752
	0.142	0.751
Standard deviation[a]	**0.034**	**0.045**
	0.036	0.048
	0.037	0.046
	0.036	0.048

[a] The theoretical mean and standard deviation (bold numbers) are estimated from the experimental data reported in [15].

$$\bar{P}(y) = \frac{1}{n_r} \sum_{r=1}^{n_r} \hat{P}_r(y) \tag{14}$$

n_r being the number of replicates (in our example, $n_r = 3$).

Following the scheme of Fig. (**1**), direct computer calculations on the same large MC samples are also performed, in order to compare the collapse load empirical distribution obtained *via* direct simulations with the one calculated *via* fitted RS models. It is worth noting that each of the 3000 MC simulations required 37 h 27 min to be performed on an Intel Pentium 3 GHz PC equipped with 1GB RAM, whereas the construction of the polynomial RS model and the evaluation of the predicted output required only 12 min.

In Fig. (**7**) we show the variability in the collapse load empirical cumulative distribution obtained from the three 3000 MC computer simulations *via* direct computer calculations, compared with the mean probability distribution.

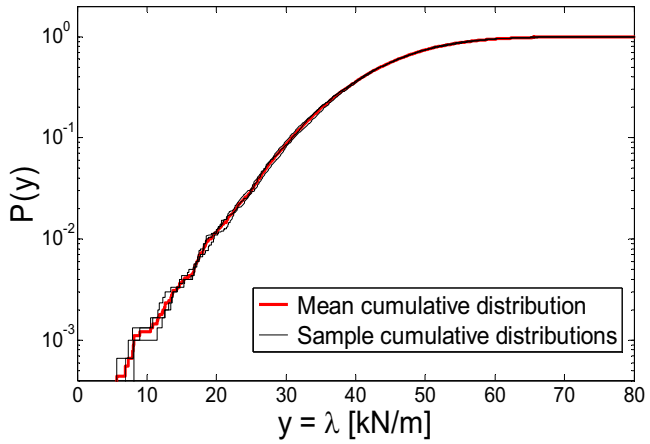

Fig. (7). Comparison of the empirical cumulative distribution from three replicated Monte Carlo samples of size 3000 with the mean empirical cumulative distribution.

On the other hand, in Fig. (**8**), the probability distributions provided by direct computer simulations and by the estimated RS models are represented. Furthermore, in the same figure, the mean percentage prediction errors $err_i(\%)$ for the RS models are depicted. As it is possible to notice from Fig. (**8**), reported in logarithmic scale along the y-axis in order to amplify the phenomenon, the RS models are able to give reliable results approximately for probability greater that 1%, thus demonstrating that the proposed approach can be used for practical applications.

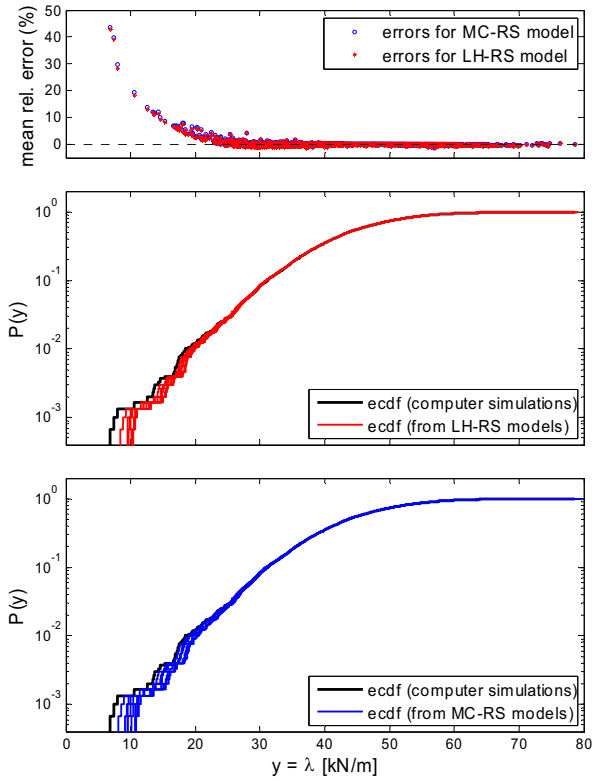

Fig. (8). Comparison of the empirical distribution functions obtained in large Monte Carlo simulations *via* direct computer simulations and *via* polynomial RS models. The theoretical cumulative distribution is also shown (dashed line). The average relative percentage error calculated on 10 replicated RS models is also shown.

As a rule, the probability distributions from RS models tend to be lower than those from direct MC simulations. This discrepancy for low collapse load values is easily justifiable by considering that, when collapse load tends to zero (i.e. when cohesion and friction angle of mortar joints are very low), a least-squares approximation used to calibrate the RS model tends to assign negligible optimization weights for low values of the collapse load (at least if such weights are compared to those relative to high values of y). On the other hand, the prediction error becomes small (i.e. below 10%) for cumulated probabilities equal or greater of 1%, which seems acceptable in practical applications.

As a final step, a comparison of the prediction accuracy of the RS models constructed on MC and LH calibration points is also examined in terms of the error measures introduced previously. As done in Ref. [21], the same three replicated large MC sets previously used to estimate the output probability distribution are used as validation points. To account for variability in RS model fitting, mean and variance of all error measures are calculated on 10 independently replicated MC-RS and LH-RS polynomials. Note that while the mean of the errors indicates the average accuracy of a RS model, the variance illustrates the variability (i.e. robustness) of the prediction accuracy [21].

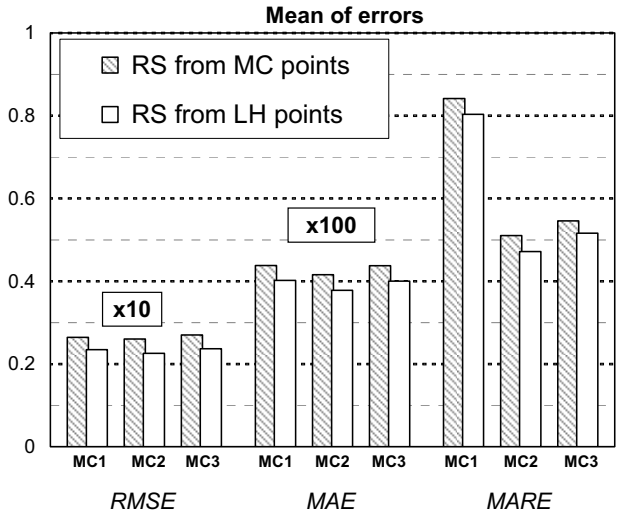

Fig. (9). Comparison of the mean of the fitting errors calculated on 10 replicated polynomial RS models constructed from MC and LH design points.

As can be seen in Fig. (**9**) and Fig. (**10**), it seems quite clear how the overall prediction accuracy of LH-RS models is almost systematically better than that of MC-RS models. In particular, LH-RS models show both an overall better accuracy (in terms of RMSE and MAE) and a best local fitting performance, quantified by MARE. In addition, LH-RS models show a better accuracy for low y values, corresponding to the left-end tail of the collapse load distribution, as confirmed by the slightly lower mean percentage error observed for low y values (see top of Fig. (**8**)).

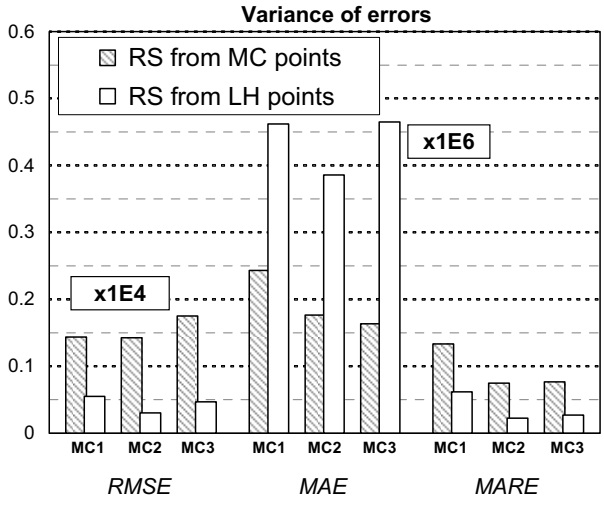

Fig. (10). Comparison of the variance of the fitting errors calculated on 10 replicated polynomial RS models constructed from MC and LH design points.

REFERENCES

[1] G. Milani, P.B. Lourenço, and A. Tralli, "Homogenised limit analysis of masonry walls. Part II: structural examples", *Comput. Struct.*, vol. 84, pp. 181-195, January 2006.

[2] G. Milani, P.B. Lourenço, and A. Tralli, "Homogenization approach for the limit analysis of out-of-plane loaded masonry walls", *J. Struct. Eng.*, vol. 132(10), pp. 1650-1663, October 2006.

[3] G. Milani, P.B. Lourenço, and A. Tralli, "3D homogenized limit analysis of masonry buildings under horizontal loads", *Eng. Struct.*, vol. 29(11), pp. 3134-3148, November 2007.

[4] P.C. Olsen, "Rigid-plastic finite element analysis of steel plates, structural girders and connections", *Comput. Meth. Appl. Mech. Eng.*, vol. 191, pp. 761-781, December 2001.

[5] S.W. Sloan, and P.W. Kleeman, "Upper bound limit analysis using discontinuous velocity fields", *Comput. Meth. Appl. Mech. Eng.*, vol. 127(1-4), pp. 293-314, November. 1995.

[6] P.C. Olsen, "Evaluation of triangular elements in rigid-plastic finite element analysis of reinforced concrete", *Comput. Meth. Appl. Mech. Eng.*, vol. 179, pp. 1-17, August 1999.

[7] D.J. Sutcliffe, H.S. Yu, and A.W. Page, "Lower bound limit analysis of unreinforced masonry shear walls", *Comput. Struct.*, vol. 79, pp. 1295-1312, June 2001.

[8] H.R. Lotfi, and B.P. Shing, "Interface model applied to fracture of masonry structures", *J. Struct. Eng.*, vol. 120, pp. 63-80, January 1994.

[9] P.B. Lourenço, R. de Borst, and J.G. Rots, "A plane stress softening plasticity model for orthotropic materials", *Int. J. Numer. Methods Eng.*, vol. 40, pp. 4033-4057, November 1997.

[10] G. Milani, P.B. Lourenço, and A. Tralli, "Homogenised limit analysis of masonry walls. Part I: failure surfaces", *Comput. Struct.*, vol. 84, pp. 166-180, January 2006.

[11] G. Magenes, and G.M. Calvi, "In-plane seismic response of brick masonry walls", *Earth. Eng. Struct. Dynamics*, vol. 26, pp. 1091-1112, November 1997.

[12] G. Milani, F.A. Zuccarello, R.S. Olivito, and A. Tralli, "Heterogeneous upper-bound finite element limit analysis of masonry walls out-of-plane loaded", *Comput. Mech.,* vol. 40(6), pp. 911-931, November 2007.

[13] P.B. Lourenço, "Anisotropic softening model for masonry plates and shells", *J. Struct. Eng.*, vol. 126(9), pp. 1008-1016, September 2000.

[14] A. Brencich, and L. Gambarotta, "Mechanical response of solid clay brickwork under eccentric loading. Part I: Unreinforced masonry", *Mater. Struct.*, vol. 38(2), pp. 257-266, March 2005.

[15] R. van der Pluijm, *Out-of-plane bending of masonry. Behaviour and strength*, PhD Thesis, Eindhoven University of Technology, 1999.

[16] M. Kobiyama, "The reduction of computational time of the Monte Carlo method, applied to radiative heat transfer with variable properties, by using a fixed properties loop", *Comput. Mech.*, vol. 5(1), pp. 33-39, January 1989.

[17] J.C. Helton, and F.J. Davies, "Latin Hypercube and the propagation of the uncertainty in analyses of complex systems", *Reliab. Eng. Syst. Saf.*, vol. 81, pp. 23-69, July 2003.

[18] P. Hradil, J. Žak, D. Novák, D. Lavicky, "Stochastic analysis of historical masonry structures", In: *Historical Constructions*, Lourenço PB, Roca P (eds), Guimarães, Portugal, November 2001.

[19] M.D. McKay, W.J. Conover, and R.J. Beckman, "A comparison of three methods for selecting values of input variables in the analysis of output from a computer code", *Technometrics*, vol. 42(1), pp. 55-61, February 2000.

[20] A.A. Giunta, and L.T. Watson, "A comparison of approximation modeling techniques: polynomial versus interpolating models", In: *7° AIAA/USAF/NASA/ISSMO Symposium on Multidisciplinary Analysis and Optimization*, St. Louis, MO, 1998, Paper AIAA: 1998-4758.

[21] R. Jin, W. Chen, and T.W. Simpson, "Comparative studies of metamodelling techniques under multiple modeling criteria", *Struct. Multidiscip. Optim.*, vol. 23, pp. 1-13, December 2001.

[22] T.W. Simpson, D.K.J. Lin, and W. Chen, "Sampling strategies for computer experiments: design and analysis", *Int. J. Rel. Appl.*, vol. 2(3), pp. 209-240, January 2002.

[23] T.W. Simpson, J.D. Peplinski, P.N. Koch, and J.K. Allen, "Metamodels for Computer-based Engineering Design: Survey and recommendations", *Eng. Comput.*, vol. 17, pp. 129–150, July 2001.

[24] L.P. Swiler, R. Slepoy, A.A. Giunta, "Evaluation of sampling methods in constructing response surface approximations", In: *47° AIAA/ASME/ASCE/AHS/ASC Structures, Structural Dynamics and Materials Conference*, Newport, Rhode Island, 2006.

[25] P. Suquet, "Analyse limite et homogeneisation", *Comptes Rendus de l'Academie des Sciences, Series IIB, Mechanics*, Vol. 296, pp. 1355-1358, 1983 [in French].

[26] K. Krabbenhoft, A.V. Lyamin, M. Hjiaj, and S.W. Sloan, "A new discontinuous upper bound limit analysis formulation", *Int. J. Numer. Methods Eng.*, Vol. 63, pp. 1069-1088, June 2005.

[27] A.A. Giunta, S.F. Wojtkiewicz, and M.S. Eldred, "Overview of modern design of experiments methods for computational simulations", In: *41° AIAA, Aerospace Sciences Meeting and Exhibit*, Reno, NV, 2003, Paper AIAA: 2003-0649.

[28] A. Florian, "An efficient sampling scheme: Updated Latin Hypercube Sampling", *Probab. Eng. Mech.*, vol. 7, pp. 123-130, Apr.-June 1992.

[29] D.E. Huntington, and C.S. Lyrintzis, "Improvements to and limitations of Latin Hypercube sampling", *Probab. Eng. Mech.*, vol. 13(4), pp. 245-253, October 1998.

[30] P. Ramu, N.H. Kim, and R.T. Haftka, "Error amplification in failure probability estimates due to small errors in response surface", *SAE paper 2007-01-0549*, 2007.

[31] A. Mood A, F. Graybill, and D. Boes, *Introduction to the theory of statistics*, McGraw-Hill, 1974.

Received: March 30, 2008 Revised: April 22, 2008 Accepted: April 22, 2008